Development of Misorientation in FCC Single Crystals Under Compression at Different Scales

D V Lychagin [1,2,3], E A Alfyorova [1] , D V Soprunov [1]

[1]Tomsk Polytechnic University
634050, Russia, Tomsk, pr. Lenina, 30
[2]Tomsk State University
634050, Russia, Tomsk, pr. Lenina, 36
[3]Tomsk State University of Architecture and Building,
634003, Russia, Tomsk, Salt sq., 2

e-mail: dvl-tomsk@mail.ru , katerina525@mail.ru

Abstract. This article presents analysis of FCC single crystals local areas reorientation under compression. The reorientation process was examined at different scales, from sample size scale to that of dislocation substructure. It has been found that disorientation in meso and macro levels is determined by accumulation of misorientation at the level of dislocation subsystem. Our research allows quantifying of accumulated misorientation magnitude. The results of this study illustrate interrelation of rotational and translational deformation modes both at the same scale level and various scale levels.

1. Introduction

During plastic deformation, there are two constantly interacting processes that specify translational and rotational components of plastic deformation. At early stages of experimental investigation of plastic deformation phenomenon, only one process was observed and described because of imperfections of research methods and facilities [e.g. 1,2].

X-ray analysis made it possible to monitor crystals' reorientation, and development of optical and electron microscopy - to observe glide dislocations. It has been established that both processes are closely related, but the reorientation is the most characteristic for large-scale plastic deformations and higher dislocation densities [3-5]. While deformation starting, changes in a defect-free crystal are performed because of dislocation glide. However, in some cases, the reorientation process can be initiated at an early stage of deformation. This phenomenon is known as twinning mechanism, which occurs if a certain crystallographic orientation, low stacking fault energy and temperature are involved.

All facts aforesaid refer to the entire range of crystalline materials, which are investigated not only by physics and chemists, but also geologists and other scientists and engineers. This approach is applicable to the study of deformation processes in single crystals with FCC lattice. Despite its apparent simplicity (no grain boundaries) single crystals are sufficiently complex objects because of anisotropy properties and aspects of symmetry. Therefore, the plastic deformation is traditionally considered at different scale levels; that enables to explore certain aspects of the phenomenon.

Investigations of plastic deformation in single crystals is important for basic science and for practical application, if extrapolating the data to a single grain of a polycrystalline aggregate or a small set of single crystals. It determines the relevance of this research. In this way, the purpose of the work is examination of misorientation development at various scale levels in relation to shearing strain processes. This phenomenon is examined in FCC samples of pure metals (aluminum, nickel, copper).

2. Materials and method

FCC single crystals (copper, aluminum, nickel) were examined. Stacking fault energy (SFE) is large enough in aluminum and nickel, so, in these materials, cross dislocation glides are rather frequent. SFE of copper is lower; however, it also has a cellular dislocation substructure within the second stage of strain hardening curves. Deformation of these materials is performed at room temperature along octahedral gliding planes. Compressive strain was performed by Instron ElectroPuls E10000 testing machine at a rate $1.4 \cdot 10^{-3}$ sec^{-1} at room temperature. Graphite lubricant was used to reduce friction force. Strain relief pictures were examined under Leica DM 2500P optical microscope and Tescan Vega II LMU raster electron microscope. To determine the misorientation of local areas electron backscatter diffraction (EBSD) attachment to a microscope Tescan Vega II LMU was used.

3. Experimental results and discussion

Let's begin examination of misorientation in single crystals with laws' descriptions starting with a macroscopic level. Crystallographic orientation changes are closely related to samples' shape changes while plastic deformation**.** The latter depends on the strain pattern and on work-piece shape to which deformation is applied. Laboratory experiments enabled us to determine a load pattern (compressive strain) and a sample form (tetragonal prism). On the one hand, factor of shape's effect on compressive strength was identified and eliminated (sample is stable with the ratio of height to width equal to two). On the other hand, deformation with friction is complicated by difference in stress condition patterns in the end faces (uneven hydrostatic compression) and the central part of the sample (uniaxial compression). Let's examine the results of experiments that were performed on samples - tetragonal prisms, subjected to compression with mechanical friction. Gliding crystallography was examined as if developing according to the systems {111}<110>. Single crystals were oriented relative to compression axis along corner lines of a standard stereographic triangle with a set of various side faces.

Previously, the authors performed systematization of strain relief structural elements, depending on crystallographic orientation of compression axes and side edges. Proportions of strain relief structural elements were determined; that clarified how zones of these elements, at macro- and meso-level, were involved in plastic deformation of investigated single crystals [6]. Magnitude of plastic deformation heterogeneity of [111] nickel single crystals was determined experimentally for examined crystallographic orientations of various side faces at various scales, considering strain relief formation and compressive stress distribution [7]. It was found that localization zones do not occur within deformation domains. Development of inner structures occurs in such a way to reduce the strain heterogeneity and approximate an average deformation value to that of local deformation. Interface areas of neighboring deformation domains and end-face deformation areas are deformation localizations areas. The domain interface area has different glide systems; in end-face areas deformation is increased because of material transfer while mechanical friction. The role of stress distribution nature in plastic deformation inhomogeneity is shown in [6,7].

We consider single crystals with a ratio of height to width equal to two. Samples with such an aspect ratio show the greatest stability under compression in the case of isotropic materials. In the case of single crystals shear anisotropy has its own individual impact. As part of the problem statement, let's examine how compression axes' and lateral faces' crystallographic orientation affect sample stability while being compressed. Various crystallographic orientations of compression axis along the long sample axis determine various resistances to deformation, depending on orientation of close-packed planes and shear directions in the volume [6]. It's been found that the greatest stability of the

sample under compression is achieved when the sample symmetry axis, relative to the compression axis, coincides with gliding systems arrangement symmetry, relative to this axis. This feature depends on the crystallographic orientation of the side faces. Besides orientation of lateral sides affects development of single crystal volume deformation and causes its discontinuity.

The most detailed investigations of deformation heterogeneity were carried out on nickel [7].

It's been found that at the macro level in single crystals with compression axis [$\overline{1}11$] deformation occurs more inhomogeneous for samples - tetragonal prisms. In this case, deformation axis orientation significantly reduces possibility of symmetric shear relative to side faces and macro-stripes forming large deformation domains. Intense folding deformation occurs in neighboring domains.

Development of compressing deformation contributes to changing in single crystals' [$\overline{1}11$] orientation; that is expressed at the macro level in sample shape curving and crystallographic reorientation of its parts.

Studies have shown that the sample body is divided several reoriented fragments [8]. A lattice orientation is less changed in the central fragment. In adjacent fragments reorientation is more pronounced. Crystal lattice orientation [$\overline{1}10$] is heavily biased. The lattice rotation occurs about the axis [110]. In end-face fragments changes of crystal lattice orientation are not observed.
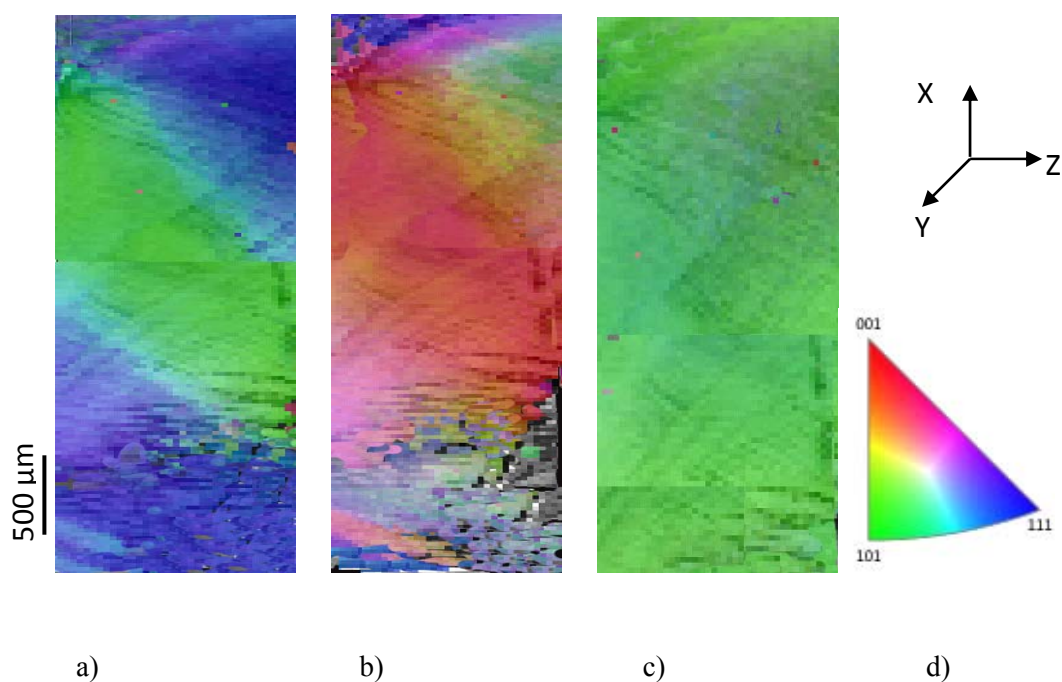

a)   b)   c)   d)

Figure 1. Formation of reorientation areas relative to axes X, Y, Z (a-c), standard stereographic triangle (d), nickel e = 22%

With further increase of strain (22%), reorientation areas' macro-fragmentation is not changed (Fig. 1). Fragments' reorientation degree increases uniformly. Crystal lattice orientation remains practically unchanged in end-face fragments. Central fragment's lattice reorients in the direction [101] relative to the deformation axis X. It's been noted that the largest reorientation areas are observed relative to the compression axis X, and almost are not observed relative to the axis Z. Such nature of reorientation in different areas of the single crystal is conditioned by several reasons. Original orientation in end-faces is permanent, if the scheme is implemented non-uniform compression due to friction, which hinders the development of deformation processes in these areas. Fragments, located on borders of regions with different stress state patterns, are reoriented the most intensively with less

deformation. This is caused by force-moment effect on a selected body, as values of stress tensor components vary in neighboring areas of this body. Reorientation is lagged in the central fragment. Reorientation of areas within single crystals of nickel, copper and aluminum occurs likewise.

Trusov's investigations [9-11] show that non-uniform stress field activates various sets of glide systems. In a local area, only one possible glide system operates in a certain time. Meanwhile, according to Taylor criterion, crystal body deformation can occur only under effect of five independent glide systems. In practice, usually, effects of more than three or four glide systems in local material volumes are not observed. In general, this is insufficient for any deformation. Therefore, this disadvantage should be compensated by reorientation of crystal areas. Based on this approach, the authors of [12] proposed a crystalline solid flow model, where disadvantage of active glide systems is complemented by rotary modes. We observe the same phenomenon in the above experiment on copper and nickel.

Compressive strain is not effective while deforming by six still loaded with shear systems in FCC single crystals with orientation of compression axis $[\bar{1}11]$ [7]. In such crystals deformation has a number of distinctive features. First, deformation occurs by shear with formation of macroscopic deformation bands systems. Second, the deformation bands systems are localized in certain areas of the crystal, which do not provide its complete deformation. Third, number and location of still loaded with shear systems do not provide orientation stability while deformation. Because of this, the single crystal is divided for disoriented fragments.

Primarily, a single crystals central area reorientation occurs. Reorientation in this body starts a mechanism of rotary deformation and also involves additional shear systems, being not active before. This is an illustrative interrelationship of translational and rotational modes of deformation on the same scale level.

Experiments prove that deformation domains should be sorted as translational and rotational ones [13]. Boundaries between of translational and rotational domains differ from grain boundaries of a polycrystalline sample. The difference is in the length and width of the boundaries, as well as in continuous transfer from one strain domain to another. In [14] authors identify these boundaries as a separate element of structural deformation with their geometric and structural parameters. Depending on domain orientation relative to applied stress, displacement deformation vectors have multidirectional or reverse directions in adjacent domains. Prevailing shearing orientation in the single crystal is always directed towards free side faces.

Areas of different deformation domains are clearly observed in the picture of displacement vectors' fields [14]. Comparison of deformation domain areas and spatial distribution of strain tensor components (shear and rotary) indicates an increase of all tensor components at the boundaries of deformation domains. This proves that increase of shear strain provides increase of rotational component. Thus, resulting deformation is higher at domains' boundary, if compared with that within a separate domain.

Data obtained with EBSD-analysis indicate accumulation of misorientation in domain boundaries. Our studies have found that misorientation increases when approaching the deformation domain boundary and significantly increases in the boundary.

Accumulation of misorientation in deformation domain depends on deformation mechanism at a meso-level. Previous studies [6] show that, depending upon single crystals' orientation, domain deformation occurs as a shearing along parallel shear planes with formation of slip bands in the form of meso- or macroscopic deformation bands. If moderate deformation degree, macroscopic deformation bands are shearing and do not lead to reorientation of mesoareas within the domain. With increase of strain degree, accumulation of dislocations' like-sign over-density occurs in local areas of the crystal, which contributes to development of misorientation. In addition, in the surface area, misorientation effect is manifested as deformation folds. Fig. 2 a-b represents the area of folds formation. EBSD-analysis is carried out in cross-section. It allows you to explore the disorientation with distance from the surface.

In this case we observe crystal local areas' reorientation in places of folds' forming. Geometric image of boundaries (Fig. 2a) illustrates distribution and magnitude of disorientation boundaries in the areas occupied by various types of structural relief elements. Color corresponds to value of misorientation angles (Fig. 2b). Here it is necessary to make a certain topical excursus. The boundaries are drawn with the program, which implies a certain disorientation interpolation on a segment, perpendicular to the boundary line. Thus, the boundaries, interpreted with the program, are diffused in a certain domain, determined by the area of interpolation. We can see that, for a given degree of deformation, disorientation angles do not exceed 5°...10°. There is disorientation magnitude to 5 ° in reoriented stripes; and larger angles along their boundaries (Fig. 2d). Consequently, folding contributes to formation of new boundaries within the single crystal.
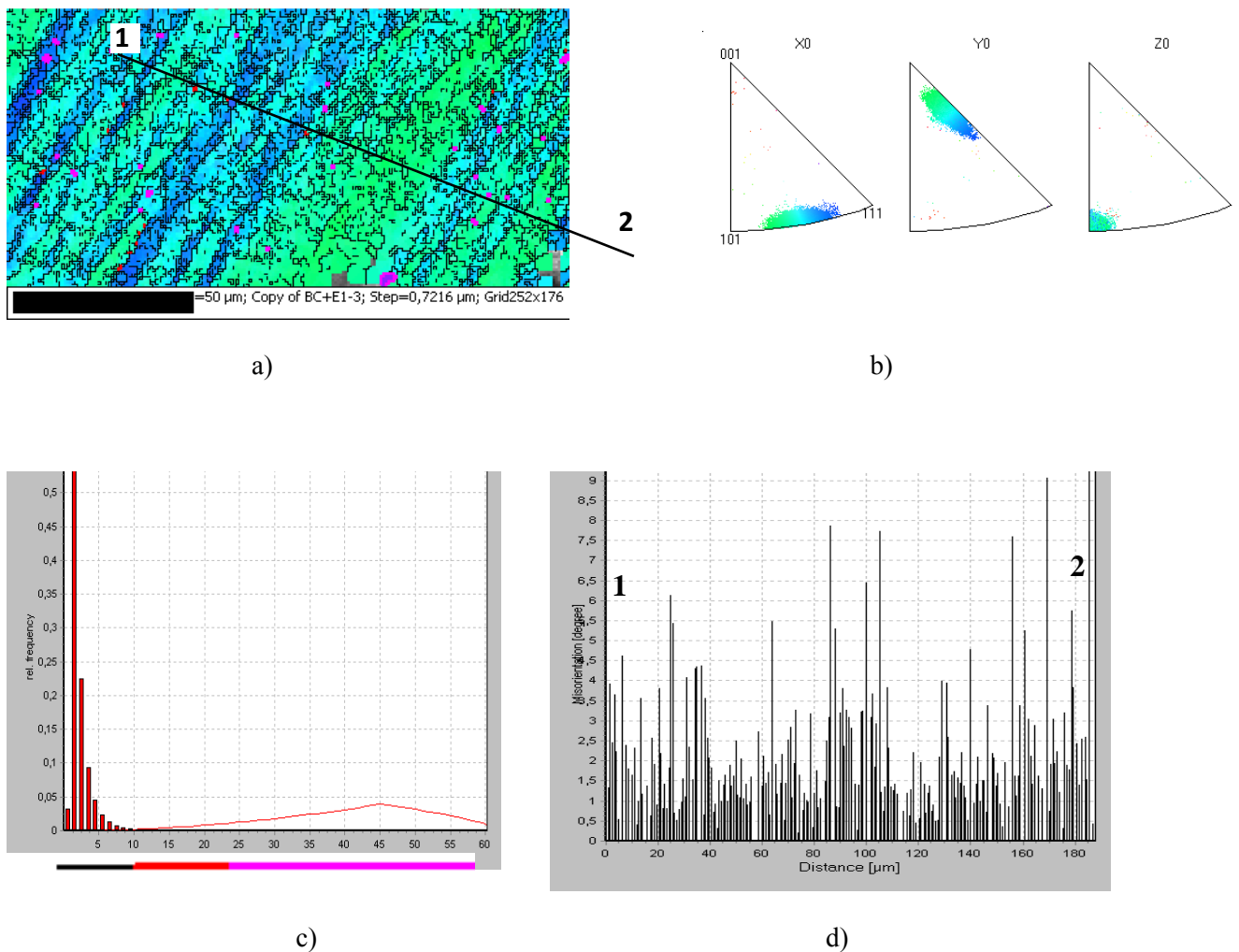

a)

b)

c)

d)

Figure 2. Geometric image of boundaries (a), standard stereographic triangle (b), frequency of angles misorientation distribution (c), transverse angles misorientation distribution 1-2 (d), Nickel, e = 16%

With use of EBSD-analysis observed disorientations were compared to disorientations of dislocation subsystem's level. EBSD record was conducted with a certain minimum grade value of 1 pixel = 5.5 microns. So, if disorientation boundary, after processing, goes along the boundary between adjacent pixels, then disorientation is at a distance of 5.5 microns. Nickel dislocation structure has the

form of dislocation cells (Fig. 3a) in the initial degree of deformation. While increase of strain, dislocation over-density is accumulated in the boundaries of dislocation cells as is evidenced by change in contrast between adjacent cells or groups of cells (Fig. 3). Contrast changes usually become apparent when disorientations' magnitudes are 0.5°. This can be verified either with electron microscope analysis or direct measuring with the goniometer, locating the tilt angle at a certain orientation of the tilt axis in the foil plane. Size of the dislocation cell is 0.5 microns at the deformation degree being examined [15]. That is, 11 dislocation cells are placed in one pixel, which give the accumulated disorientation 5.5° observed in the experiment. Thus, EBSD-defined misorientation magnitude agrees with that of disorientation, accumulated during deformation in cellular dislocation substructure.
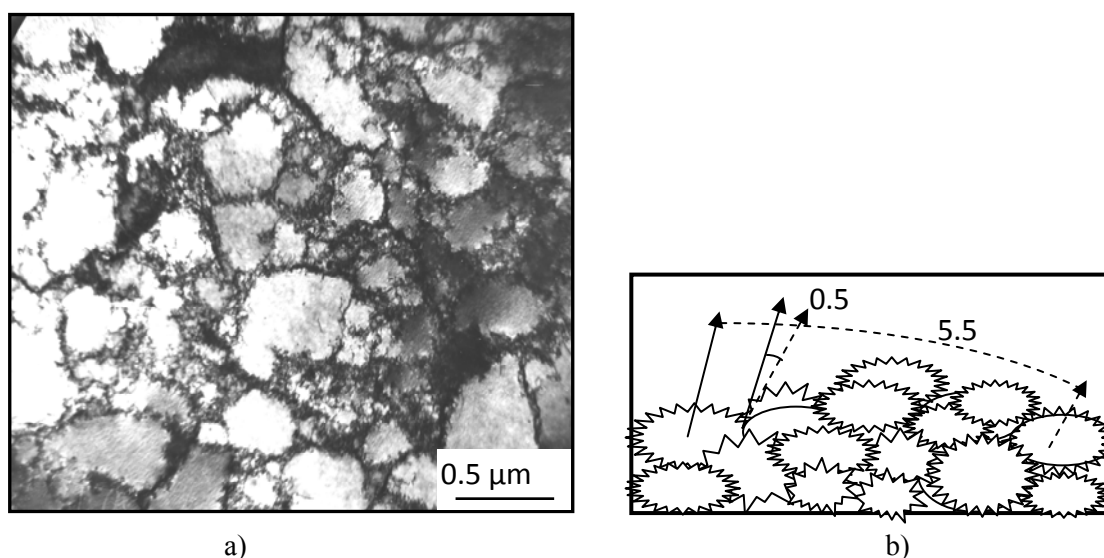

a)   b)

Figure 3. Cellular dislocation substructure (a) and its misorientation accumulation diagram (b)

Over-density accumulation varies in cell walls of finite thickness. Depending on like-sign dislocations' distribution at the boundary, it has various magnitudes of disorientation while transitioning across the boundary; and transforms sequentially into blocked, fragmented and then sub-grain structure. Volumes, bounded with disorientations, constitute structure elements which can be subjected to reorientation under certain conditions. In fact, it occurs, in particular, under conditions of material super-plastic flow, when the grain boundary gliding or microporosity formation facilitates rotation of grains in the boundary.

At meso-level, individual rotational defects of very significant magnitudes can be observed, mainly those of disclination type. There are many studies that interpret phenomena in the dislocation structure as manifestations of disclination formations. By now, findings of investigations, obtained while experimenting with metallic materials, are incomplete. It is our belief that a disclination loop, experimentally obtained (by authors), is rather valuable; the loop was formed in iron-nickel ordered alloy with compression axis orientation [001] [16]. Magnitude of azimuthal disorientation, determined by splitting of reflexes on an electron diffraction pattern, is 10 °. In this case, disclination loop formation facilitated "knife-edge" shear boundary formation in the rest of the crystal volume, which resulted in a shift of dislocation cell wall by 0.2 ... 0.4 micron. Earlier authors classified this phenomenon as a mechanism for destruction of stable cellular structure of the ordered alloy. The experimental results also illustrate interrelation of translational and rotational deformation modes at the level of mesodefects of the dislocation-disclination subsystem. Deformation mechanism is a parallel action of two "knife-like" edges, which share cell boundaries in opposite directions. After the

strong shear ceases, within the crystal a large-scale disclination loop is formed; which has a large misorientation angle between loop interior part and surrounding matrix.

4. Conclusions

Thus, analysis of scientific papers and authors' own results show interrelation of disorientation processes at different scale levels. Accumulation of misorientation at dislocation subsystem's level (lower scale level) leads to accumulation of misorientation at meso- and macro-levels. Our research allows quantifying of accumulated misorientation magnitude and monitoring of crystallographic orientation changes in deformation elements at all scales. Furthermore, the results of this study illustrate interrelation of rotational and translational deformation modes both at the same scale level and various scale levels.

Acknowledgements

References

[1] Honeycombe R W K 1984 *The Plastic Deformation of Metals*. Edward Arnold & American Society of Metals, London.
[2] Higashida K, Takimura J, Narita N 1986 *Mater. Sci. Eng.* **81** 239.
[3] Ke-Shen Cheonga, Esteban P Busso 2006 *Journal of the Mechanics and Physics of Solids* **54** 671
[4] Koneva N A, Zhukovskiy S P et al. 1985 *Physics of Metals and Metallography* **60 1** 157.
[5] Hatherly M 1982 *Strength Met. and Alloys. In: Proc. 6th Int. Conf., Melbourne*, Oxford, **2** 1181.
[6] Lychagin D V 2006 *Phys. Mesomech.* **9** 3-4 95.
[7] Lychagin D V, Alfyorova E A, Starenchenko V A 2011 *Phys. Mesomech.* 14 (1-2), 66.
[8] Lychagin D V, Tarasov S Yu, Chumaevskii A V, Alfyorova E A 2015 *International Journal of Plasticity* **69** 36.
[9] Trusov P V, Volegov P S, Shveykin A I 2013 *Computational Materials Science* **79** 429.
[10] Trusov P V, Shveykin A I, Nechaeva E S, Volegov P S 2012 *Physical Mesomechanics* **15 3-4** 155.
[11] Trusov P V, Shveykin A I 2013 *Physical Mesomechanics* **16 1** 23.
[12] Arul Kumar M, Mahesh S 2012 *International Journal of Plasticity* **36** 15.
[13] Teplyakova L A, Kozlov E V 2006 *Physical Mesomechanics* **9 1-2** 53.
[14] Kibitkin V V, Solodushkin A I et al. 2011 *Optoelectronics, Instrumentation and Data Processing* **47** 4 83
[15] Starenchenko V A, Shaekhov R V et al. 1999 *Russ. Phys. J.* **42 7** 653.
[16] Teplyakova L A, Koneva N A et al. 1988 *Russ. Phys. J.* **31 2** 18.